Heliyon 9 (2023) e20311

Contents lists available at ScienceDirect

Heliyon

journal homepage: www.cell.com/heliyon

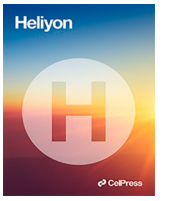

A study of the magnetic properties of $LaNi_5$ and their effect on hydrogen desorption under theaction of a magnetostatic field

Sihem Belkhiria [b,*], Chaker Briki [b], Mohamed Houcine Dhaou [a,b,**], Faisal Alresheedi [a], Abdelmajid Jemni [b]

[a] Department of Physics, College of Science, Qassim University, Buraidah, 51452, Saudi Arabia
[b] University of Monastir, Faculty of Sciences, Laboratory of Thermal and Energetic Systems Studies, LR99ES31, 5019, Monastir, Tunisia

ARTICLE INFO

Keywords:
Hysteresis cycle
Thermo-magnetic effect
Magnetization at saturation
Desorption reaction
Hydrogen storage
Reaction kinetics

ABSTRACT

A study of the magnetic properties of $LaNi_5$ intermetallic compoundand and their effect on desorption reaction was carried out as a function of temperature. A Vibrating Sample Magnetometer (VSM) was used for the magnetic measurements and a Metal Hydrogen Reactor (MHR) supplied by a constant current through a coil was used for the hydrogen desorption reaction under the action of a magnetostatic field. Then, the hysteresis cycle, the first magnetization curve, the thermo-magnetization curves and the desorbed hydrogen mass were determined. The results showed that the application of a magnetic field corresponding to the magnetization at saturation M_s at a given temperature improved the hydrogen desorption reaction by the $LaNi_5$.

1. Introduction

World energy consumption will grow by 28% between 2015 and 2040 [1]. Therefore, in response to the depletion of fossil fuels and the rising need for energy, researchers have created innovative methods for energy storage. By the way, fossil fuels are predicted to make up only a small percentage of the world's power generation by 2050, while renewable energy sources will continue to meet the primary and secondary energy needs [2]. Hydrogen is a particularly fascinating renewable and extremely powerful energy vector [3]. Nevertheless, before being used, hydrogen must be stored. Already, to develop a hydrogen-storage technology, critical considerations must be taken into account such as the storage density, safety, affordability, and service life [4]. Although it can be stored in liquid or gas form, hydrogen can be conveniently stored in a solid state by physisorption or chemisorption particularly in metal hydrides form [5]. Thus, the discovery of hydrogen storage in metal hydrides by the $LaNi_5$ [6–9]and the FeTi [10–12]compounds offered new possibilities for hydrogen storage technologies. Intermetallic compounds are still at the center of interest from researchers since they provided an attractive combination of low price and high hydrogen storage density under predetermined circumstances. In these compounds, hydrogen penetrates the metal network and shares its electron with the conduction strip of the intermetallic or metallic element. This interaction allows the formation of a metallic bond between the metal and hydrogen [13]. The intermetallic compound $LaNi_5$ and its derivatives are known for their hydrogen storage capacities since they reversibly store hydrogen at moderate temperature and pressure without special activation treatment [14–16]. However, the development of $LaNi_5$ hydride, as a hydrogen storage material has remained at the basic stage and has not really moved towards concrete applications. This limitation is due to the hydride's

* Corresponding author.
** Corresponding author.
E-mail addresses: sihembelkhiria@yahoo.fr (S. Belkhiria), m.dhaou@qu.edu.sa (M.H. Dhaou).

https://doi.org/10.1016/j.heliyon.2023.e20311
Received 22 August 2023; Received in revised form 18 September 2023; Accepted 19 September 2023
Available online 21 September 2023

low mass storage capacity, compared to magnesium hydride for example, because of its low thermal conductivity. In fact, to be marketed, a storage material must combine a high hydrogen storage capacity under standard pressure and temperature conditions via light and bulky tanks with an acceptable storage cost. To improve the heat and mass transfer within the hydride bed, several experimental and numerical research works have been carried out. Scientists have used several methods including controlled substitution. Improving the storage capacity of the $LaNi_5$ compound through the addition of other metals such as Sn, Fe, Al, Co, etc.. to give the material new properties is common [17–21]. The majority of these studies have demonstrated that the substituted compounds do not have the same properties as the parent compounds. However, the hydrogen storage capacity did not improve sufficiently.

Over and above, several research works focused on improving heat transfer within the hydride bed by using new metal-hydrogen reactors (MHR) configurations [22–25]. These studies are examined how different MHR setups performed in relation to a number of operating conditional variables, including hydrogen inlet design, input pressure, and cooling / heating fluid temperature. Then, for better efficiency, MHR have been equipped with various forms of inner and outer heat exchangers [26–29]. Thereby, heat exchangers are used to accelerate the heat transfer rate in the metal hydride bed. Besides, an important way to enhance the storage reaction is by adding fins to heat exchangers. Thence, heat pipes given a better heat transfer by more than 50% compared to heat exchangers [30,31].

Another way to improve the hydrogen storage reaction is to use a phase change material (PCM) [32–34]. Researchers have shown that using the appropriate phase change material is an attractive option for storing or supplying heat during absorption or desorption, eliminating the need for high temperature level waste heat.

Even if all these techniques have shown an improvement in the reversible hydrogen storage properties by metal hydrides, they still limited by the heat losses by convection and conduction along a long and heavy heating installation marked by unpleasant storage conditions. Additionally, the problem which arises by implementing any of these techniques is the increased thermal mass of the system, which affects the hydrogen storage capacity.

To solve the above mentioned problems, hydrogen storage under the effect of an external magnetic field (electromagnetic and magnetostatic field) by the $LaNi_5$ compound attracts recently the attention of researchers. Firstly, Electromagnetic induction (EMI) during desorption reactions has been proposed experimentally as a new heating technique [35]. Then, a numerical simulation has been carried out to study the performance of the MHR using the EMI [36]. The EMI heating technique has shown spectacular results. In fact, the kinetics of the reaction has been improved by more than 80%. The applied electromagnetic field offered an attractive combination of efficiency, speed, and economy of energy and space.

Moreover, the effects of an applied magnetostatic field and of the thermo-magnetization properties on the hydrogen storage reaction are of great interest. In fact, the study of the effect of magnetic transitions caused by the application of external magnetic fields and their variation with hydrogen storage has attracted the attention of several researchers [37–39]. Aware that the $LaNi_5$ is an intermetallic compound of a 3d magnetic transition; it is a Pauli paramagnet compound [40–43], researchers noted that the hydrogenation considerably affects the magnetic properties of hydrides due to the increase in mesh volume and the change in the magnetic structure marked by the segregation of ferromagnetic particles (Ni) [44–47]. Particularly, the change in the magnetic properties, which occur due to the hydrogen absorption / desorption has prompted researchers to study the effect of an external magnetostatic field on the hydrogen storage reaction. Although the magnetic properties of AB_5 and their derivative intermetallics are widely studied by scientists [48–50], few published works have considered the effect of the magnetic properties on the hydrogen storage reaction by the $LaNi_5$.

In a previously published work [51], the effect of a weak external field (less than 0.03T) on the hydrogen absorption/desorption reaction was investigated. Results showed that the applied magnetostatic field improves the absorption reaction for low temperatures and that the magnetostatic field has no effect on the desorption reaction.

In this paper, we present the results of the magnetic properties of the $LaNi_5$ intermetallic as a function of the applied temperature and external magnetic field and their effect on the hydrogen desorption reaction when the applied magnetostatic field is up to 0.1 T. The intriguing hydrogen storage properties of $LaNi_5$, such as its large hydrogen storage capacity, straightforward activation, and safety of the hydrogen storage procedure, were the primary reasons for choosing this material for the proposed study [52]. Then, it is because of its fascinating magnetic properties at which temperature variation and particle size have a significant impact. In fact, although experimental results state $LaNi_5$ as a paramagnetic material [53], several studies showed that it can exhibit properties of a very weak ferromagnetic material. In addition, when exposed to a magnetic field, it manifests the formation of ferromagnetic particles of nickel [54]. The presence of nickel in $LaNi_5$ introduces a magnetic behavior of the material. The magnetic moments of nickel atoms are influenced and controlled through the application of an external magnetostatic field. Understanding the impact of magnetism on hydrogen desorption kinetics provides insights into optimizing the material's performance for hydrogen storage. Lastly, $LaNi_5$ was chosen due to its commercial accessibility.

2. Experimental steps

2.1. Alloy preparation

30g of $LaNi_5$ alloy (99.9% purity) was ground into a fine powder by mechanical grinding. This step took 2 h. To prevent the sample's temperature from rising too much during the grinding process, there would be a 5 min break every 15 min. This step is crucial on the one hand, to prepare the intermetallic to reversibly store the hydrogen by increasing its surface and subsequently facilitating its activation. On the other hand, to prepare it to undergo the effect of the magnetic field by decreasing, the size of the particles and stimulating the segregation of Ni particles on the metal surface.

The surface states of the obtained powders were then verified using a Scanning Electron Microscope (SEM) before and after

grinding (Fig. 1(a and b)) and studied by X-ray diffraction (RX) (Fig. 2).

The obtained results showed that the grains of the crushed compound were finer, had a particle size less than 1.5 μm, and had a regular shape, which facilitates the activation process during the hydrogen absorption-desorption cycles.

Fig. 2 shows the appearance of the X-ray diffraction profiles of the crystallographic structure of the $LaNi_5$ alloy before the absorption-desorption processes of hydrogen. From this figure, it is observed that the compound $LaNi_5$ crystallizes in the hexagonal $CaCu_5$ structure with the space group $P6_3/mmc$ and with the lattice parameters of the mesh: a = b = 5.019 Å and c = 3.982 Å.

2.2. Hydrogen storage reaction

The experimental device and the alloy preparation steps are described in our previous published works [51]. The hydrogen tank was connected to the reactor with connection tubes and valves. The hydride bed was cooled or heated by heating water coming from the thermostatic bath. A pressure sensor was installed inside the hydrogen tank to control the variation of the hydrogen pressure (Fig. 3). It is connected to an acquisition card installed on a micro computer to visualize the evolution of the pressure during the absorption and desorption reaction.

Hydrogen absorption reaction steps.

* The tank was supplied with hydrogen at a pressure of 6 bar.
* The heat transfer fluid of the thermostatic bath was cooled at a temperature of 300 K.
* The hydrogen tank was put in contact with the reactor. Then, the hydrogen passed transiently from the tank to the reactor until reaching stability.
* The connection between the tank and the reactor was closed and the tank was re-energized with a pressure of 6 bar and the absorption was repeated in the same conditions.

Hydrogen desorption reaction steps.

* The hydrogen tank was emptied using a vacuum pump up to a pressure of 0.1 bar.

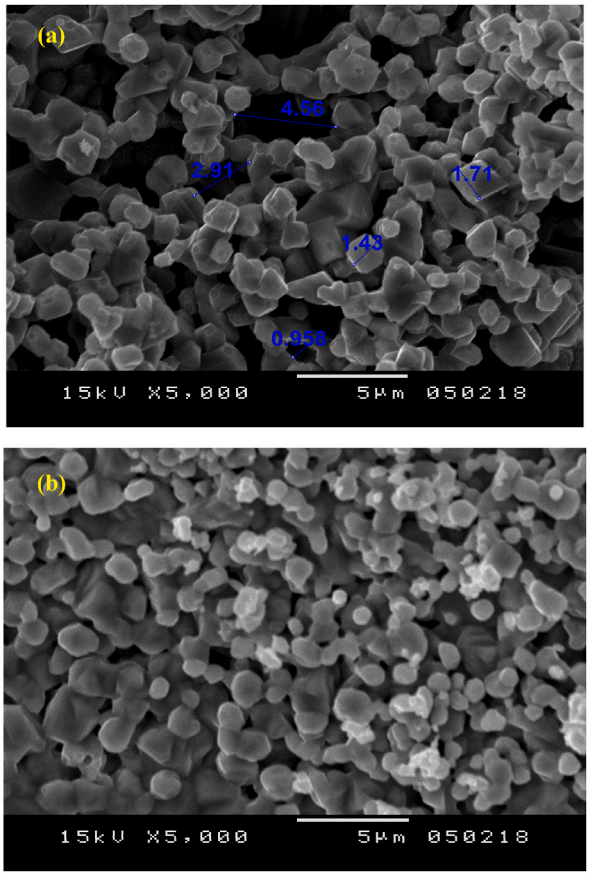

Fig. 1. (a,b): SEM of the $LaNi_5$ before grinding (a) and after grinding (b).

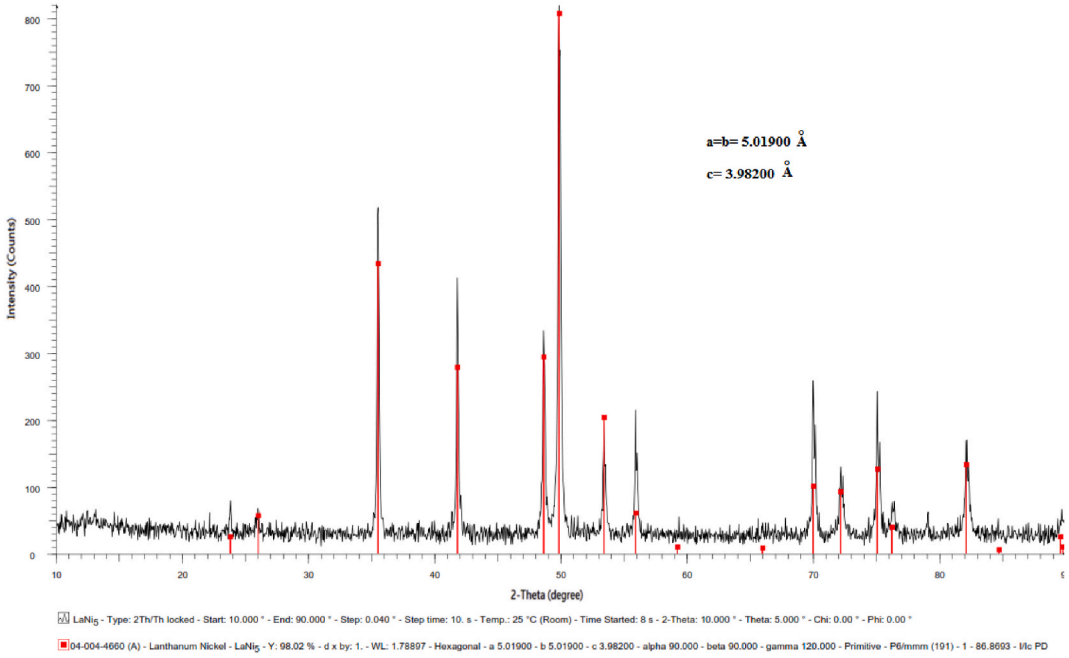

Fig. 2. The XRD profiles for $LaNi_5$ before hydrogenation [55].

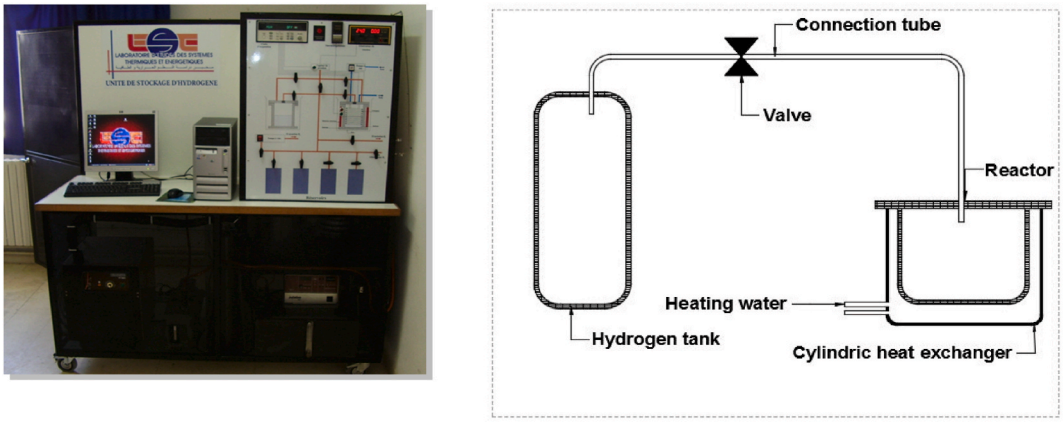

Fig. 3. Experimental device: Metal-Hydrogen reactor (MHR).

* The hydride bed was heated until reaching a temperature of 333 K.
* The hydrogen tank was put in contact with the hydrogen reactor. The hydrogen passed, in these conditions, into the tank, until reaching stability.
* The connection between the tank and the reactor was closed; the hydrogen tank was emptied until reaching 0.1 bar and desorption was repeated until the same conditions.

2.3. The magnetic field production during desorption

The hydrogen metal reactor was equipped with a coil of 128 turns and a length L = 24 mm, traversed by a direct current delivered by a power supply unit to produce a constant magnetic field around the hydride bed.

3. Results

3.1. Magnetic hysteresis cycle

The hysteresis cycle at room temperature (300 K) versus the applied magnetic field of the crushed $LaNi_5$ intermetallic compound is shown in Fig. 4.

The hysteresis cycle had three distinct zones.

* First zone: it is a linear zone. In fact, when the field increased the magnetization increased too. However, the increase due to magnetization was very slow compared to that in the field.
* Second zone: This zone is characterized by a remarkable variation of the magnetization against zero field.
* Third zone: it is a saturation region for which magnetization hardly changed against a remarkable variation of the field.

The hysteresis cycle at room temperature shows that the material is a weak ferromagnetic material classified as magnetically soft. It is characterized by a weak magnetization at saturation (Table 1) with a non large cycle [56–59].

This is particularly the case in certain compounds comprising two types of atoms with different magnetic moments of spin. Therefore, all magnetic moments of the same type tend to go in one direction and those of the other type in the opposite direction, which results in a non-zero spontaneous magnetization. Although there are studies which have supported these findings and considered that $LaNi_5$ as a weak ferromagnetic compound [60,61], others have observed a ferromagnetic behavior of the $LaNi_5$ [62].

The magnetic measurement parameters of the $LaNi_5$ intermetallic found from the hysteresis cycle are in Table 1.

3.2. Magnetization curves as a function of the applied field

3.2.1. Magnetization curves for the $LaNi_5$ at constant temperature

Fig. 5 shows the first magnetization curve at room temperature (300 K). The material is initially demagnetized (no magnetization). The progressive increasing in the applied field caused the gradual increase in magnetization.

The magnetization curve of the $LaNi_5$ intermetallic consists of three parts.

* A linear region for which the magnetization acquired by the intermetallic increases according to the applied field.
* Saturation bend for which the variation of the magnetization as a function of the field was very slow.
* A saturation region for which the increase in the applied field had no effect on magnetization.

From a demagnetized state (H = 0) applying a regularly increasing magnetic field of excitation leads to the appearance of a magnetic induction M (H). The energy of coupling with the external environment promotes a growth in the volume of the favorably oriented domains. The maximum magnetization, M_s, known as saturation, corresponds to a perfect alignment of all the atomic moments on the applied field. The magnetic parameters from the curve of the first magnetization are shown in Table 2.

The average value of magnetization at saturation M_s measured experimentally by the VSM magnetometer from the virgin magnetization curve was around 0.15 emu/g. The M_s was reached from a magnetic field of 1 T. The required magnetic field H_s to reach $0.7M_s$ is around 0.12 T (**Table 2**). This value was reached from the saturation bend region and it depends on the temperature.

3.2.2. Isotherms and isofields magnetization measurement below curie point

Fig. 6-a shows the magnetization isofield when H = 1T versus temperatures. Below 200 K, the magnetization decreased when

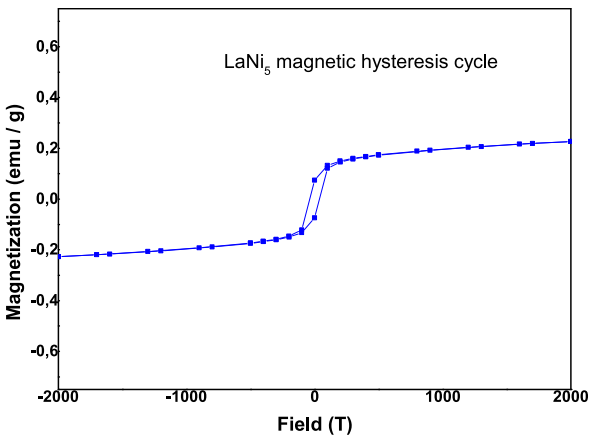

Fig. 4. Hysteresis cycle at room temperature for the $LaNi_5$intermetallic compound.

Table 1
Magnetic parameters of the $LaNi_5$ from experimental hysteresis cycle at room temperature.

Hysteresis loop	Avarage	Parameters definitions
H_c (Oe)	44.297	Coercitive field: field at wich M/H change sign
M_r (emu/g)	$42{,}186*10^{-3}$	Ramanent magnetization: M at H = 0
M_s (emu/g)	0.2	Saturation magnetization: maximum M measured
Susceptibility χ_0 (emu/g)	0.17	Magneic susceptibility calculated from slope

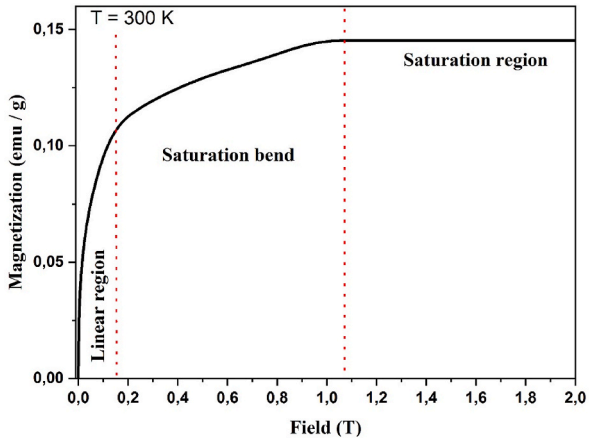

Fig. 5. First Magnetization curve as a function of the applied field at room temperature for the $LaNi_5$intermetallic compound.

Table 2
Magnetic parameters at room temperature of the $LaNi_5$ from the first experimental magnetization curve.

Magnetization parameters	Avarage	Parameters definitions
$H_{0.5}$ (T)	0.0384	H at M = 0.5 M
Ms (emu/g)	0.15	Saturation magnetization: maximum M measured
H_s (T)	0.12	Field at which M (H) reaches 0.7 M

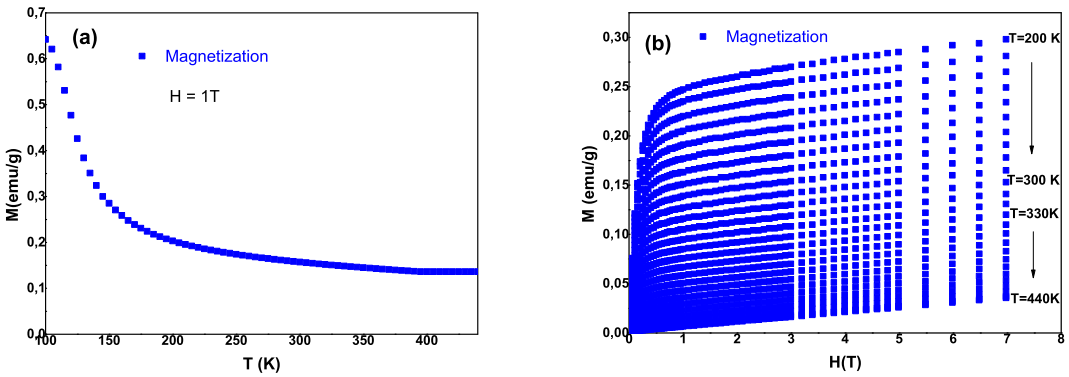

Fig. 6. Magnetization isofield at different temperatures (a) and magnetization isotherms at different field's (b) measurements for the $LaNi_5$ compound.

temperatures increased.

The decrease in magnetization as a function of temperature led to an increase in the magnetic entropy (eq. (1)) [63–65]**:**

$$-\Delta S_M = \int_0^H \left(\frac{\partial M}{\partial T}\right)_H dH \tag{1}$$

Above 200 K, the increase in temperature has no effect on the magnetization when the applied magnetic field is constant (1T). Fig. 6-b shows the magnetization isotherms of the $LaNi_5$ intermetallic as a function of the magnetic field at constant temperatures. It

is observed that the saturation magnetization decreased with temperature increase. As well, for higher temperatures, the $LaNi_5$intermetallic compound requires higher fields to reach the magnetization at saturation. Indeed, the high temperature attenuates the magnetization at saturation and subsequently destroys the magnetic order [66,67]**.** The magnetic order induced by the stabilization of magnetization can be useful to improve the performance of reversible hydrogen storage reaction within the $LaNi_5$ intermetallic. We propose in what follows to study the hydrogen desorption reaction under the effect of a precisely selected magnetic field.

3.3. Application: hydrogen desorption reaction under magnetic field

3.3.1. Pressure and mass saturation into the hydride bed

The pressure (Fig. 7-a) and mass (Fig. 7-b) variations were studied during successive absorption cycles at a pressure of 6 bar and a temperature of 300 K while pressure (Fig. 8-a) and mass (Fig. 7-b) variations of the desorption cycles were studied at a pressure of 0.1 bar and a temperature of 333 K. Absorption and desorption cycles were repeated until the pressure of stored or released hydrogen stabilizes (see Fig. 9).

Under these experimental conditions, the number of cycles required to reach saturation by the $LaNi_5$ is 4 cycles. In fact, after 4 successive absorptions cycles, the amount of the absorbed hydrogen remains constant. Then, the totality of the absorbed hydrogen is released after 4 successive desorptions.

Successive cycles of reversible hydrogen storage by the $LaNi_5$ intermetallic lead to the decrease of the particle size and the segregation of the Ni ferromagnetic particles. In fact, numerous investigations have demonstrated that an increase in the amount of Ni nanoparticles leads to an increase in the ferromagnetic contribution, which rises with the number of hydrogenation cycles. Approximately 1% Ni precipitated after 102 cycles [58–61]. Therefore, in order to prepare the alloy to react with the external magnetic field, the operation of consecutive absorption-desorption is generated many times at the same initial pressure and temperature conditions.

3.3.2. Variation of magnetization during hydrogen desorption reaction

Fig.9 shows the magnetization versus hydrogen mass desorbed in the desorption processes at 303 K. The objective of this measurements was to determine the effect of desorbed hydrogen on magnetization.

It is shown that the magnetization immediately increases from a negative minimum value M_{min} to a positive maximum value M_{max} when the desorption process is triggered. Moreover, it is composed mainly of two maxima marked by the presence of two peaks. The first peak corresponds to the decrease in magnetization from its maximum value $M_{max} = 0.18$ emu/g to a lower value 0.13 emu/g. This is explained by the fact that the system's temperature decreases as a result of the endothermic character of the desorption reaction when the hydrogen atoms start to depart the metallic matrix's interstitial during α phase. Then, the rise of the magnetization to its maximum value M_{max}, marked by the second peak, is attributed to the heating process by hot water from the thermostatic bath (section 2.2). After this magnetic relaxation the magnetization returns to decrease gradually until a state of equilibrium is attained corresponding to β-phase. It can therefore be concluded that the α and β phases have distinct magnetic properties. This result is confirmed by Ref. [68]. This difference is explained by the variation of the microstructure and the thermal effect during the desorption reaction. Therefore, in transition-metal alloys, the absorbed hydrogen is present as metal hydride and soluble hydrogen atoms. Every free one electron is carried by each hydrogen atom, and this electron can change the magnetic moment of an alloy. The magnetic moment will rise if the hydrogen electrons have the same spin as the vast majority of d-band electrons in the alloy. When the electrons have the opposite spin, there is a reduction in the magnetic moment [69,70].

3.3.3. Effect of the magnetostatic field on the hydrogen desorption

The performances of the desorption reaction were tested at three different temperatures (303 K, 333 K and 343 K), with an initial pressure in the reactor of 0.1 bar, at zero field and at a field of 0.1T and 0.15T, 0.1T and 0.15T. These fields were chosen since the band of magnetization at saturation revolves around them ($H_{0.5}$ and H_s) for the considered temperatures **(**Table 2**).**

Fig. 10 shows the effect of temperature on the desorption reaction at zero field (a) and in the presence of a magnetic field of 0.15 T (b).

At zero field, the increase in the applied temperature improved the mass and the kinetics of desorption because of the endothermic nature of the reaction. However, at an applied external magnetic field it is observed that the mass of desorbed hydrogen was higher at $T = 303$ K than the mass desorbed at $T = 333$ K and at $T = 343$ K. This can be explained by the significant desorbed mass enhancement posed by the applied magnetic field at $T = 303$ K against a weak improvement at 333 K and 343 K. It can be concluded that $LaNi_5$ alloy shows good desorption kinetics under the effect of the applied magnetic field compared to cooling water circulation. This suggests that the applied magnetic field is a more effective method for enhancing the kinetics of the hydrogen desorption reaction in $LaNi_5$. As the magnetic field interacts with the magnetic moments of the nickel atoms in the $LaNi_5$ lattice, it leads to a distortion of the crystal structure, resulting in an expansion of the unit cell.

Fig. 11, 12 and 13show the effect of the applied magnetostatic field at different temperatures.At 303 K (Fig. 11), the applied magnetic fields considerably improved the desorbed hydrogen mass.

At 333 K and 343 K (Fig. 12 and Fig. 13), the applied field of 0.1T had no effect on reaction. Whereas, a field of 0.15 T improved desorption. This improvement is more observable at lower temperature (333 K). This is explained by the fact that higher temperatures require stronger fields to reach the saturation of magnetization.

The applied field of 0.15 T is in the region of the saturation bend (Fig. 6). In this region a certain magnetic order is established, which improves of the reaction.

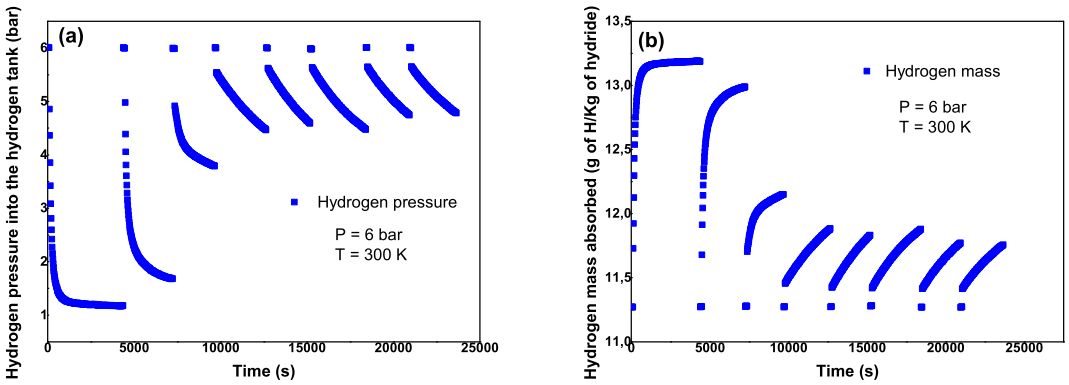

Fig. 7. Pressure (a) and mass (b) variations during 8 successive absorption cycles until reaching saturation.

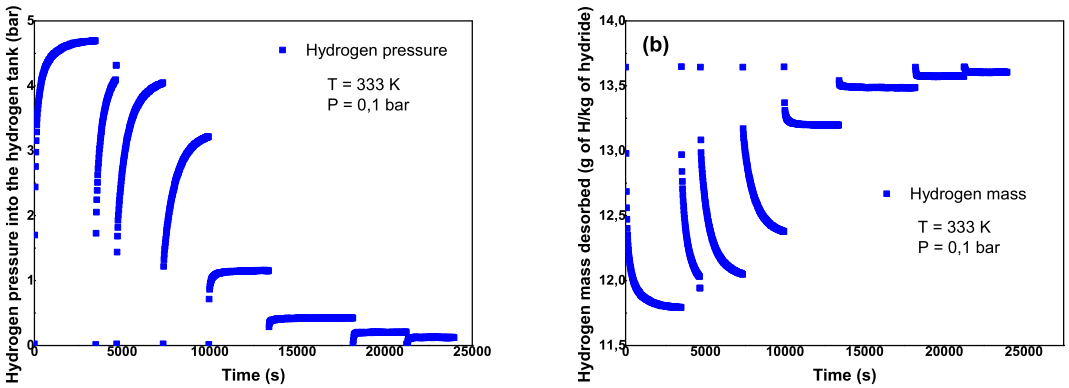

Fig. 8. Pressure (a) and mass (b) variations during 8 successive desorption cycles until reaching saturation.

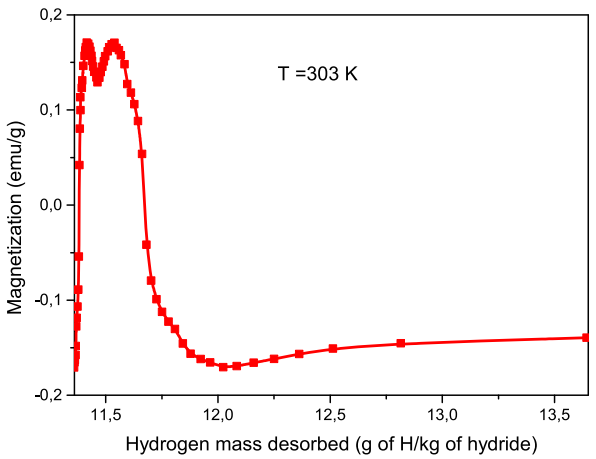

Fig. 9. Magnetization as a function of hydrogen mass desorbed.

4. Conclusion

The magnetic properties of the $LaNi_5$ compound have been studied. The hysteresis cycles and the magnetization curves as a function of the applied field and the temperature were determined. In the one hand, it is shown from the magnetization curves that the crushed $LaNi_5$ intermetallic is weakly ferromagnetic at room temperature due to surface segregation into Ni and La oxide, and that the ferromagnetic contribution rises with the number of hydrogenation cycles.

In the other hand, the thermo-magnetic measurements and the variation of magnetization during desorption have shown that

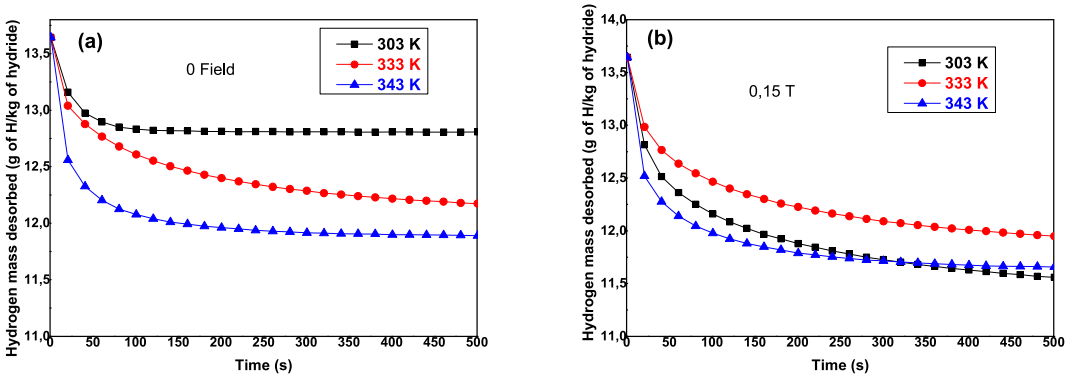

Fig. 10. Effect of the temperature on the hydrogen desorption reaction by the $LaNi_5$ at zero field (a) and at a non-zero field (b).

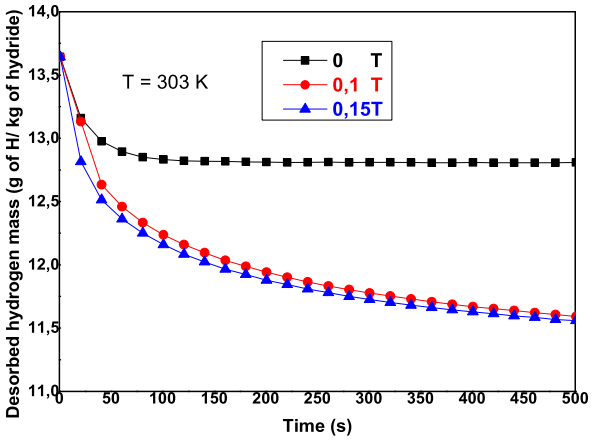

Fig. 11. Effect of the applied magnetic field on the desorption reaction at T = 303 K.

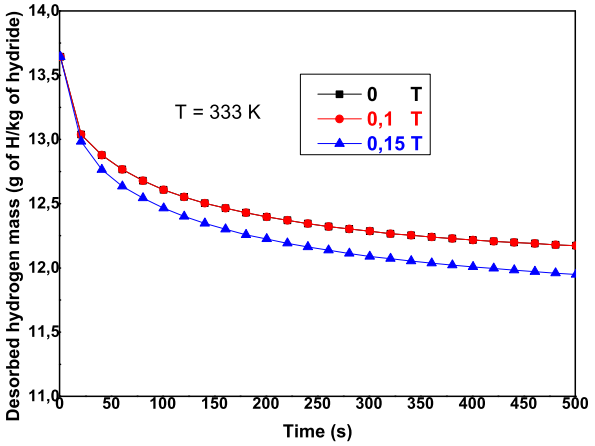

Fig. 12. Effect of the applied magnetic field on the desorption reaction at T = 333 K.

magnetic properties vary depending on the microstructure and the thermal effect. Therefore, based on these findings, the effect of the magnetic properties on the hydrogen desorption reaction as a function of the applied temperature and magnetostatic field in $LaNi_5$ hydride has been studied. The results have shown that, at a given temperature, the applied field corresponding to the bend of magnetization at saturation improves the desorption reaction and that the magnetic order imposed by the field out weighs the effect of the increase of the applied temperature.

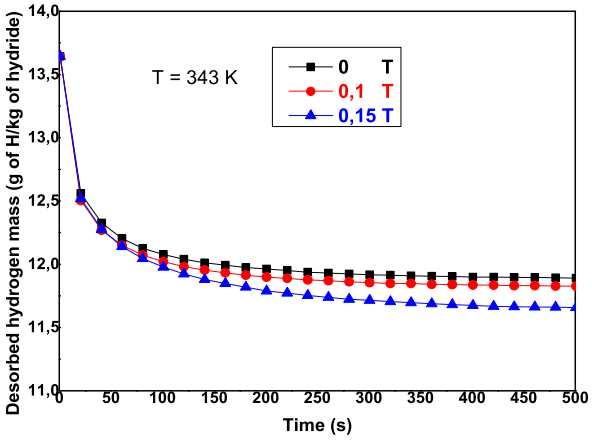

Fig. 13. Effect of the applied magnetic field on the desorption reaction at T = 343 K.

Author contribution statement

Sihem Belkhiria: Conceived and designed the experiments; Performed the experiments; Analyzed and interpreted the data; Contributed reagents, materials, analysis tools or data; Wrote the paper. Chaker Briki: Analyzed and interpreted the data; Wrote the paper. Mohamed Houcine Dhaou: Performed the experiments; Contributed reagents, materials, analysis tools or data. Faisal Alresheedi: Analyzed and interpreted the data. Abdelmajid Jemni: Conceived and designed the experiments; Wrote the paper.

Data availability statement

Data will be made available on request.

Declaration of competing interest

The authors declare that they have no known competing financial interests or personal relationships that could have appeared to influence the work reported in this paper.

Acknowledgements

Researchers would like to thank the Deanship of Scientific Research, Qassim University for funding publication of this project.

References

[1] T. Ahmad, D. Zhang, A critical review of comparative global historical energy consumption and future demand. the story told so far, Energy Rep. 6 (2020) 1973–1991.
[2] S. Ali, A. Elmuez, A. Dhay, A. Waleed, S. Masoud, Progress on nano-scaled alloys and mixed metal oxides in solid-state hydrogen storage; an overview, Int. J. Hydrogen Energy 46 (2023) 31699–31726.
[3] H. Robert, V. Annamaria, V. Yee, J. Jiří, K. Damjan, C. Lidija, Hydrogen Production, Storage and Transport for Renewable Energy and Chemicals: an Environmental Foot Print Assessment, Renewable and Sustainable Energy Reviews173, 2023, 113113.
[4] T.P. Yadav, A. Kumar, S.K. Verma, N.K. Mukhopadhyay, High-entropy alloys for solid hydrogen storage: potentials and prospects, Transactions of the Indian National Academy of Engineering 7 (2022) 147–156.
[5] Q. Hassan, A. Sameen, H. Salman, M. Jaszczur, A. Khudhair Al-Jiboory, Hydrogen energy future: advancements in storage technologies and implications for sustainability, J. Energy Storage 72 (2023), 108404.
[6] V. Van, F. Kuijpers, H. Bruning, Reversible room-temperature absorption of large quantities of hydrogen by intermetallic compounds, Philips research report 25 (1970) 133–140.
[7] B. Jose, A. Jose-Ramon, B. Jussara, B. Marcello, B. Craig, C. Giovanni, G. Noris, M. David, N. Matylda, J. Isaac, H. Emil, J. Torben, J. Julian, K. Thomas, V. Mykhaylol, M. Kandavel, M. Amelia, P. Julian, S. Sabrina, A. Drew, S. Alastair, W. Gavin, J. Colin, Y. Heena, Y. Volodymyr, Z. Andreas, D. Martin, Application of hydrides in hydrogen storage and compression: achievements, outlook and perspectives, Int. J. Hydrogen Energy 44 (2019) 7780–7808.
[8] S. Louis, Z. Andreas, Hydrogen-storage materials for mobile applications, Insight review articles 414 (2001) 338–344.
[9] K. Manmeet, K. Kaushi, Review on hydrogen storage materials and methods from an electrochemical viewpoint, J. Energy Storage 23 (2019) 234–249.
[10] J. Reilly, R. Wiswall, Formation and properties of iron titanium hydride, Inorg. Chem. 13 (1974) 218–222.
[11] H. Liu, J. Zhang, P. Sun, C. Zhou, Y. Liu, Z. Fang, An overview of TiFe alloys for hydrogen storage: structure, processes, properties, and applications, J. Energy Storage 68 (2023), 107772.
[12] V. Livramento, C. Rangel, J. Correia, N. Shohoji, R. Silva, Synthesis of FeTi hydrogen storage material via ball milling: effect of milling energy and atmosphere, International Workshop Advances on Fuel Cells and the Hydrogen Economy (2008).
[13] U. Eberle, G. Arnold, R. Helmolt, Hydrogen storage in metal–hydrogen systems and their derivatives, J. Power Sources 154 (2006) 456–460.
[14] G. Liang, J. Huot, R. Schulz, Hydrogen storage properties of the mechanically alloyed LaNi5-based materials, J. Alloys Compd. (2001) 133–139.
[15] A. Busra, I. Mustafa, C. Selahattin, Experimental analysis of hydrogen storage performance of a LaNi5–H2 reactor with phase change materials, Int. J. Hydrogen Energy 48 (2023) 6010–6022.

[16] C. Atef, D. Aissa, N. Leila, M. Slimane, Chapter 19 - upscaling of LaNi5-based metal hydride reactor for solid-state hydrogen storage: numerical simulation of the absorption–desorption cyclic processes, Green Approach to Alternative Fuel for a Sustainable Future 57 (2023) 269.
[17] Y. Hongen, W. Yong, C. Shunpeng, X. Zewei, W. Yiman, C. Nuo, Y. Xue, L. Wei, X. Lei, L. Xingguo, Z. Jie, Pd-modified LaNi5 nanoparticles for efficient hydrogen storage in a carbazole type liquid organic hydrogen carrier, Appl. Catal. B Environ. 317 (2022), 121720.
[18] J. Jose, R. Daniel, F. Ricardo, S. Juliano, B. Wagner, T. Tomaz, S. Claudio, J. Walter, Hydrogen storage in MgH_2-$LaNi_5$ composites prepared by cold rolling under inert atmosphere, Int. J. Hydrogen Energy 43 (2018) 13348–13355.
[19] G. Oliva, M. Fuentes, E.M. Borzone, G.O. Meyer, P. Aguirre, Hydrogen storage on LaNi5−xSnx. Experimental and phenomenological Model-based analysis, Energy Convers. Manag. 173 (2018) 113–122.
[20] Z. Zhida, Z. Shuai, L. Haoqi, W. Jie, Y. Kai, C. Honghui, L. Jingjing, Stability of LaNi5-*x*Co*x* alloys cycled in hydrogen — Part 1 evolution in gaseous hydrogen storage performance, Int. J. Hydrogen Energy (2019) 15159–15172.
[21] K. Sarath, A. Kumar, S. Srinivasa, Thermochemical energy storage using coupled metal hydride beds of Mg-LaNi5 composites and LaNi5 based hydrides for concentrated solar power plants, Appl. Therm. Eng. 219 (2023), 119521.
[22] C. Briki, S. Belkhiria, H. Dhaou, F. Askri, A. Jemni, Dynamic study of a new design of a tanks based on metallic hydrides, Int. J. Hydrogen Energy 43 (2018) 1566–1576.
[23] A. Souahlia, H. Dhaou, F. Askri, S. Mellouli, A. Jemni, S. Ben Nasrallah, Experimental and comparative study of metal hydride hydrogen tanks, Int. J. Hydrogen Energy 36 (2011) 12918–12922.
[24] P. Muthukumar, M. Maiya, S. Murthy, Experiment on a metal hydride-based hydrogen storage device, Int. J. Hydrogen Energy 30 (2005) 1569–1581.
[25] A.K. Aadhithiyan, K.V.J. Bhargav, R. Sreeraj, S. Anbarasu, Multi-objective design optimization of hydride hydrogen storage reactor structured with finned helical tubes based on energetic and economic analyses, J. Energy Storage 64 (2023), 107194.
[26] H. Dhaou, A. Souahlia, S. Mellouli, F. Askri, A. Jemni, S. Ben Nasrallah, Experimental study of a metal hydride vessel based on a finned spiral heat exchanger, Int. J. Hydrogen Energy 35 (2010) 1674–1680.
[27] H. Dhaou, N. Ben Khedher, S. Mellouli, A. Souahlia, F. Askri, A. Jemni, S. Ben Nasrallah, Improvement of thermal performance of spiral heat exchanger on hydrogen storage by adding copper fins, Int. J. Therm. Sci. (2011) 2536–2542.
[28] A. Souahlia, H. Dhaou, F. Askri, S. Mellouli, A. Jemni, S. Ben Nasrallah, Experimental study and characterization of metal hydride containers, Int. J. Hydrogen Energy 36 (2011) 4952–4957.
[29] A. Souahlia, H. Dhaou, S. Mellouli, F. Askri, A. Jemni, S. Ben Nasrallah, Experimental study of metal hydride-based hydrogen storage tank at constant supply pressure, Int. J. Hydrogen Energy 39 (2014) 7365–7372.
[30] A. Fawzi, M. Elhamshri, K. Muhammet, Enhancement of hydrogen charging in metal hydride-based storage systems using heat pipe, Int. J. Hydrogen Energy 34 (2019) 18927–18938.
[31] C.A. Chung, Y. Chen, Y. Chen, M. Chang, CFD investigation on performance enhancement of metal hydride hydrogen storage vessels using heat pipes, Appl. Therm. Eng. 91 (2015) 434–446.
[32] Y. Yang, Y. Yi, L. Jianfeng, D. Jing, W. Weilong, Y. Jinyue, Enhanced hydrogen storage of a LaNi5 based reactor by using phase change materials, Renew. Energy 180 (2021) 734–743.
[33] C. Atef, M. Slimane, G. Noureddine, B. Yacine, Thermodynamics and kinetics analysis of hydrogen absorption in large-scale metal hydride reactor coupled to phase change material-metal foam-based latent heat storage system, Int. J. Hydrogen Energy 64 (2022) 27617–27632.
[34] A. Busra, I. Mustafa, C. Selahattin, Experimental analysis of hydrogen storage performance of a LaNi5–H2 reactor with phase change materials, Int. J. Hydrogen Energy 48 (2023) 6010–6022.
[35] S. Belkhiria, C. Briki, M.H. Dhaou, N. Sdiri, A. Jemni, F. Askri, S. Ben Nasrallah, Experimental study of metal–hydrogen reactor behavior during desorption under heating by electromagnetic induction, Int. J. Hydrogen Energy (2017) 16645–16656.
[36] A. Talal, A. Salem, F. Askri, Numerical investigation on performance enhancement of metal-hydride hydrogen tank using electromagnetic induction heating, Appl. Therm. Eng. (2023), 120072.
[37] B. Franco, A. Colin, Secondary alkaline cells. Modern Batteries (Second Edition) An Introduction to Electrochemical Power Sources (1997) 162–197.
[38] M. Afshari, Structural and magnetic properties of $LaNi_5$ and $LaNi_{3.94}Al_{1.06}$ alloys, before and after hydrogenation, Superconductivity and Novel Magnetism 30 (2017) 2255–2259.
[39] S. Belkhiria, C. Briki, M.H. Dhaou, F. Alresheedi, J. Abdelmajid, Magnetic and hydrogen storage properties under the action of a sinusoidal electromagnetic field by the $LaNi_{3.6}Al_{0.4}Co_{0.7}Mn_{0.3}$ alloy, Journal of Pure and Applied Mathematics 7 (2023) 219–225.
[40] S. Reza, A. Hadi, P. Faiz, Structural, morphological, magnetic and hydrogen absorption properties of $LaNi_5$ alloy: a comprehensive study, Int. J. Mod. Phys. B 28 (2014), 1450079.
[41] A. Mehdi, H. Mohammad, Experimental Study of Structural and Magnetic Properties of LaNi5 and MmNi4.7Al0.3 Hydrogen Storage Alloys, Journal of Superconductivity and NovelMagnetism32, 2019, pp. 1853–1857.
[42] J. Jean, B. Valérie, C. Fermín, Z. Junxian, L. Michel, $LaNi_5$ related AB_5 compounds: structure, properties and applications, J. Alloys Compd. 862 (2021), 158163.
[43] I. Tereshina, S. Veselova, V. Verbetsky, M. Paukov, D. Gorbunov, E. Tereshina-Chitrova, Influence of substitutions and hydrogenation on the structural and magnetic properties of $(R'R'')_2Fe_{17}$ (R', R'' = Sm, Er, Ho): compositions with promising fundamental characteristics, J. Alloys Compd. 897 (2022), 163228.
[44] Y. Knyazev, Y. Kuz'min, A. Lukoyanov, A. Kuchin, Optical properties and electronic structure of $LaNi_{(5-x)}Cu_x$ (x=0-1,2) intermetallic system, Journal of Solid State Phenomena (2011) 168–169, 529-532.
[45] S. Nkosi, B. Yalisi, D. Motaung, J. Keartlandb, E. Sideras-Haddadb, A. Forbes, B. Mwakikunga, Antiferromagnetic–paramagnetic state transition of NiO synthesized by pulsed laser deposition, Appl. Surf. Sci. 265 (2013) 860–864.
[46] M. Spodaryk, N. Gasilova, A. Züttel, Hydrogen storage and electrochemical properties of $LaNi_{5-x}Cu_x$ hydride-forming alloys, J. Alloys Compd. 775 (2019) 175–180.
[47] M. Komeilia, H. Arabia, R. Yusupovc, S. Ghorbanib, F. Vagizovc, F. Pourarian, The effect of hydrogen pressure on magnetic properties of $Zr_2(Co_{0.5}Fe_{0.2}Ni_{0.2}V_{0.1})$ alloy, J. Alloys Compd. 927 (2022), 167025.
[48] T. Blach, E. Gray, Magnetic properties of the LaNi5–H system, J. Alloys Compd. 254 (1997) 336–338.
[49] S. Shahin, H. Mary, K. Sarada, The effect of magnetic field on thermal-ReactionKinetics of a paramagnetic metal hydride storage bed, Appl. Sci. 7 (2017) 1006.
[50] M.J. Jean, P.B. Valérie, C.J. Fermín, M.L. Zhang, $LaNi_5$ related AB_5 compounds: structure, properties and applications, J. Alloys Compd. (2021), 158163.
[51] S. Belkhiria, C. Briki, M.H. Dhaou, A. Jemni, Experimental study of a metal –hydrogen reactor behavior's subjected under the action of an external magnetostatic field during absorption and desorption, Int. J. Hydrogen Energy 45 (2020) 4673–4684.
[52] G. Kenta, H. Tomoyuki, Y. Isao, N. Wataru, Suitability evaluation of $LaNi_5$ as hydrogen-storage-alloy actuator by in-situ displacement measurement during hydrogen pressure change, Molecules 24 (13) (2019) 2420.
[53] F. Alam, S. Matar, M. Nakhl, N. Ouaini, Investigation of changes in crystal and electronic structures by hydrogen within $LaNi_5$ from first-principles, Solid State Sci. 11 (2009) 1098–1106.
[54] F. Albertini, F. Canepa, S. Cirafici, E. Franceschi, M. Napoletano, A. Paoluzi, L. Pareti, M. Solzi, Composition dependence of magnetic and magnetothermal properties of Ni-Mn-Ga shape memory alloys, Journal of Magnetic and Magnetsm Materials272– 276 (2004) 2111–2112.
[55] C. Briki, P. de Rango, S. Belkhiria, M.H. Dhaou, A. Jemni, Measurements of expansion of $LaNi_5$ compacted powder during hydrogen absorption/desorption cycles and their influences on the reactor wall, Int. J. Hydrogen Energy 44 (2019) 13647–13654.
[56] M. Peter, Magnetism in the solid state: an introduction, Encyclopedia of Materials: Sci. Technol. 134 (2006) 5018–5032.
[57] A. Salwa, A. Mohamed, E. Ashraf, Magnetic properties of nanoparticles glass–ceramic rich with copper ions, J. Non-Cryst. Solids 357 (2011) 3888–3896.
[58] D. Gatteschi, Magnetic Molecular Materials, Current Opinion in Solid State and Materials Science1, 1996, pp. 192–198.
[59] L. Schlapbach, Magnetic Properties of $LaNi_5$ and Their Variation with Hydrogen Absorption and Desorption, Journal of Physics F: Metal Physics10, 2000, p. 2477.

[60] M. Afshari, Structural and magnetic properties of LaNi5 and LaNi3.94Al1.06 alloys, before and after hydrogenation, Journal of Superconductivity and Novel Magnetism 30 (2017) 2255–2259.
[61] M. Afshari, M. Amerioun, Experimental study of structural and magnetic properties of LaNi5 and MmNi4.7Al0.3, Hydrogen Storage Alloys. Journal of Superconductivity and Novel Magnetism 32 (2019) 1853–1857.
[62] J. Alvarez, R. Valenti, The antiferromagnetic/paramagnetic transition in mixed-spin compounds R_2BaNiO_5. The European physical, Journal 44 (2005) 439–445.
[63] K. Ondrej, Z. Adriana, H. Pavol, T. Róbert, Z. Vladimír, The study of entropy change and magnetocaloric response in magnetic nanoparticles via heat capacity measurements, Int. J. Refrig. (2018) 107–112.
[64] M.S. Anwar, H.K. Bon, Observation of the magnetic entropy change in Zn doped $MnFe_2O_4$ common ceramic: Be cool being environmental friendly, Curr. Appl. Phys. (2022) 77–88.
[65] B. Sardar, A. Imtiaz, S. Marzougui, A. Farhat, Entropy analysis in single phase nanofluid in square enclosure under effectiveness of inclined magnetic field by executing finite element simulations, Geoenergy Science and Engineering (2023), 211483.
[66] L. Zu, S. Lin, Y. Liu, J. Lin, B. Yuan, X. Kan, P. Tong, W. Song, P. Sun, A first-order antiferromagnetic-paramagnetic transition induced by structural transition in $GeNCr_3$, Appl. Phys. Lett. 108 (2016), 031906.
[67] T. Blach, A. Mac, E. Gray, Magnetic properties of the LaNi–H system, J. Alloys Compd. 253–254 (1997) 336–338.
[68] D. Vaughan, Magnetic and electrostatic separation, Mineral Processing Design and Operations (Second Edition (2016) 629–687.
[69] B. Cullity, Introduction to Magnetic Materials, Addison-Wesley, Reading, 1972, p. 134.
[70] P. Termsuksawad, S. Niyomsoan, R. Goldfarb, V. Kaydanov, D. Olson, B. Mishra, Z. Gavra, Measurement of hydrogen in alloys by magnetic and electronic techniques, J. Alloys Compd. 373 (2004) 86–95.